Aromatic Sulfur-Nitrogen Extraction using Ionic Liquids: Experiments and Predictions using an *a priori* Model

Ramalingam Anantharaj
Dept. of Chemical Engineering, University of Malaya, Kuala Lampur 50603, Malaysia

Tamal Banerjee
Dept. of Chemical Engineering, Indian Institute of Technology Guwahati, Guwahati 781039, Assam, India

DOI 10.1002/aic.14224

The tie-line composition of three quaternary system namely 1-ethyl-3-methylimidazolium acetate ([EMIM][OAc]) ([EMIM][OAc]) (1) + thiophene (2) + pyridine (3) + toluene (4), 1-ethyl-3-methylimidazolium ethylsulphate ([EMIM][EtSO$_4$]) (1) + thiophene (2) + pyridine (3) + toluene (4), 1-ethyl-3-methylimidazolium methylsulphonate ([EMIM][MeSO$_3$]) (1) + thiophene (2) + pyridine (3) + toluene (4) were experimentally determined at 298.15 K. The measured tie-line data were successfully correlated with the nonrandom two liquid and UNIversal QUAsiChemical model prediction which gave less than 1% root mean square deviation (RMSD). [EMIM][MeSO$_3$] looks to be a promising solvent for the simultaneous separation having distribution ratios less than unity for both thiophene and pyridine. The quantum chemical-based conductor like screening model for real solvent (COSMO-RS) model was then used to predict the tie-line composition of quaternary systems. COSMO-RS gave the RMSD for the studied systems to be 8.41, 8.74, and 6.53% for the ionic liquids, respectively. © 2013 American Institute of Chemical Engineers *AIChE J*, 59: 4806–4815, 2013

Keywords: ionic liquids, simultaneous extraction, quaternary systems, COSMO-RS model, molecular models

Introduction

Sulfur and nitrogen compounds in diesel oil leads to SO$_X$ and NO$_X$ emission to air and strongly inhibit the performance of pollution control equipment[1–4]on vehicles. The emission of such compounds contributes to ozone formation[5] and acid deposition.[6,7]Thus increasing regulatory measures are forced on refineries to reduce nitrogen and sulfur containing compounds in diesel oil. The regulations proposes that the upper limit of nitrogen containing compounds in diesel to be reduced from >75 to <1 ppm[8–10] and sulfur containing compounds from 500 to <10 ppm.[8–10] However, the hydrodesulfurization and hydrodinitrification are unable to reduce the aromatic sulfur and nitrogen.[9,11] These compounds do not react with active catalyst, even under severe operating conditions which requires high energy consumption. Further, the aromatic sulfur and nitrogen compounds inhibits the role of catalyst.[6]

Liquid–liquid extraction (LLE) is an efficient process as compared to distillation, absorption, and other chemical process for the removal of aromatic sulfur and nitrogen containing compounds from diesel oil.[12–14] The main advantages of LLE as compared to other separation processes are ambient temperature and atmospheric pressure,[15] no additional catalyst,[15,16] and low energy consumption.[2] In addition, the hydrogen consumption and handling are also eliminated.[2] The aromatic nitrogen and sulfur atom posses sterical hindrance.[17,18] Therefore, the active site of such compounds can be enhanced by choosing a solvent having an opposite behaviour in the mixture. In contrast to organic solvents, ionic liquids (ILs) have enormous advantages with respect to green chemical processes.[2] This includes negligible vapor pressure, nonflammability, high thermal and chemical stability, high ionic conductivity, wide liquid range, good solubility with organic and inorganic compounds, and higher density than organic solvent and water. Thus, the IL exists as two phases when in contact with aliphatic hydrocarbons and aromatic compounds.[7,10,12,14]

ILs can be regenerated after multiple extractions without additional equipment or operation. Further, ILs does not affect the chemical structure of the diesel compounds as well as cetane number of the diesel oil.[2,19] However, in a recent work,[20] it was found that the regeneration of ILs is difficult for a LLE operation involving nitrogen species. In their work, toluene was used as a regenerative solvent to remove indole and dibenzothiophene (DBT) from 1-ethyl-3-methylimidazolium chloride. It was found that the extent of removal was 46% (from initial concentration 2993 mg/kg IL) after two regenerative cycles for indole and nearly 85% (from initial concentration 4532 mg/kg IL) for DBT. Further, chlorine-based IL (i.e., Cl and AlCl$_3$) are highly sensitive with moisture/air and water and produces HF and HCl[4] due to their poor hydrolysis stability. Thus, they do not act as green solvent, as it releases toxic and corrosive HF into the environment. Conversely, their cost is very high as compared to halogen-free anions like alkyl sulfate, alkyl borate, and alkyl acetate. The quantum chemical-based model (COSMO-RS) has also indicated that halogen-free anions possess high selectivity, capacity, and performance index for the removal of aromatic sulfur and nitrogen compounds from diesel oil.[9,11]

Correspondence concerning this article should be addressed to T. Banerjee at tamalb@iitg.ernet.in.

The present work investigates the ability and feasibility of imidazolium-based IL for simultaneous desulfurization and denitrification of diesel oil where diesel oil is represented by an aromatic compound, that is, toulene. Earlier work[4] does not discuss about simultaneous removal of thiophene and pyridine, but only discusses its extraction explicitly and individually with thiophene and pyridine. Research group worldwide reports the removal of sulfur and nitrogen from diesel oil using anion such as tetrafluoroborate [BF_4], chlorine [Cl], hexafluorophosphate [PF_6], and bis{(trifluoromethyl) sulfonyl} imide[Tf_2N]. However, with the production of HF/HCl, the handling of IL with these anions are not easy, and there are issues which are difficult to handle such as stability and corrosion using halogen containing ILs. Thus, this research focuses on the use of completely halogen free ILs as suggested by Mochizuki et al.[21] and Eber et al.[22] Further, Domanska et al.[23] reported that the alkyl sulfate anion-based ILs is much superior when compared to other popular anions as tetrafluoroborate [BF_4], chlorine [Cl], hexafluorophosphate [PF_6]. This also agrees with our earlier findings based on COSMO-RS predictions.[9,11,24] It was shown from our previous work that a smaller cation like [EMIM] gave higher selectivity.[25] Also via COSMO-RS the anions such as [OAc],[$EtSO_4$], and [$MeSO_3$] gave high values of selectivites. Our results show that allkylsulfate and acetate anion-based ILs are the best one suited for the simultaneous removal of thiophene and pyridine. In addition, the anions are also less viscous and hydrolytically stable.

With these points in mind, we have chosen the ILs; 1-ethyl-3-methylimidazolium acetate ([EMIM][OAc]), 1-ethyl-3-methylimidazolium ethylsulphate ([EMIM][$EtSO_4$]), and 1-ethyl-3-methylimidazolium methylsulphonate ([EMIM][$MeSO_3$]). The experimental LLE tie-line data were evaluated for the above mentioned systems from which the selectivity and distribution coefficient were calculated. The reliability of experimental data was validated using the nonrandom two liquid (NRTL) and UNIversal QUAsiChemical (UNIQUAC) model and the results were analyzed in terms of root mean square deviation (RMSD) values between experimental and predicted tie lines. Further, quantum chemical-based COSMO-RS model was used to predict the tie lines.

Computational Theory

NRTL and UNIQUAC model

NRTL[26] and UNIQUAC[27] models have been successfully used for the IL-based ternary LLE predictions.[10,28] The two models were applied to predict the tie-line composition of ILs + thiophene + pyridine + toluene-based quaternary systems. From the experimental data, the binary interaction parameters τ_{ij} and/or A_{ij} were calculated by the minimization of the objective function as given below. Here, τ_{ij} is the interaction between component i and j for NRTL model. The details of the model and the minimization procedure can be obtained from our previous work.[10,29–31]

$$\text{Maximize}: F\left(\begin{array}{l}\text{with respect to } A_{ij}\\ \text{where } i,j=1,2,3\\ \text{and } j\neq i\end{array}\right)=-\sum_{k=1}^{m}\sum_{l=I}^{II}\sum_{i=1}^{c}w_{ik}^{l}\left(x_{ik}^{l}-\hat{x}_{ik}^{l}\right)^{2},\quad w_{ik}^{l}=1, \tag{1}$$

For UNIQUAC model prediction, the pure component parameters such as r and q were calculated on the basis of solvent excluding surface concepts.[32]

COSMO-RS model

The COSMO-RS model[33,34] has provided great influence on the thermodynamics properties of fluid and its mixtures properties, especially where the experimental data are limited. This model requires only the molecular structure as input. The details of COSMO-RS are given in our previous work.[35–37] For the IL modeling, COSMO-RS solves the problem in either of the three steps: (a) the metafile, (b) ion-pair approach, and (c) the electro neutral approach.[38] We have used metafile approach in which the ions are treated separately in the quantum chemical COSMO calculation, and the IL is described as the sum of sigma profile, area, and volume of the cation and anion. This sigma profile provides the charge distribution over the molecular surface which is required in order to calculate the molecular interaction energies such as misfit (E_{misfit}), hydrogen bond (E_{HB}), and van der Waals(E_{vdW}) interactions. The screening charges can be obtained from first principles solvation calculation of the molecule in a perfect conductor known as COSMO calculation. In the COSMO calculation, the surface of a molecule is dissected in small segments and screening charges are determined for each segment such that the net potential everywhere at the surface is zero (perfect screening). The screening charge of the molecular surface is then stored in a COSMO file. Hence the total interaction can be defined as

$$E_{\text{int}}=E_{\text{misfit}}+E_{\text{vdW}}+E_{\text{hb}} \tag{2}$$

The three-dimensional screening charge density distribution is quantified using histogram known as σ-profile $p(\sigma)$, which is the probability of finding a surface segment with screening charge density σ, that is, $p(\sigma)=\frac{A_i(\sigma)}{A_i}$, where $A_i(\sigma)$ is the surface area with a charge density of value σ and A_i is total surface area of species i. The σ-profile for the mixture is determined from the area weighted average of contributions from all its components, that is,

$$p_s(\sigma)=\frac{\sum_i x_iA_ip_i(\sigma)}{\sum_i x_iA_i} \tag{3}$$

Therefore, the final result of the distinct COSMO calculations of the ions is combined into one file and termed as metafile. The sigma profiles for the thiophene, pyridine, and toluene molecules are generated using the same methodology. The compositions of the extract and raffinate phases are calculated using a flash algorithm as described by the modified Rashford–Rice Algorithm (Figure 1)[31] which requires the activity coefficient at isothermal conditions. The quality of prediction is given via RMSD values, that is,

$$\text{RMSD(in\%)}=\left(-\frac{F}{2mc}\right)^{1/2}=\left[\sum_{k=1}^{m}\sum_{i=1}^{c}\sum_{l=I}^{II}\frac{\left(x_{ik}^{l}-\hat{x}_{ik}^{l}\right)^{2}}{2mc}\right]^{1/2}\times 100 \tag{4}$$

where, m and c refers to the number of tie lines and components (viz. (4) for the present system). The experimental and predicted composition values are indicated by x_{ik}^{l} and $\hat{x}_{ik}^{l}$ for component i for the kth tie line in phase l, respectively.

Experimental section

The ILs: 1-ethyl-3-methylimidazolium acetate [EMIM][OAc] ($C_8H_{14}N_2O_2$) of purity > 99% and 1-ethyl-3-methylimidazolium

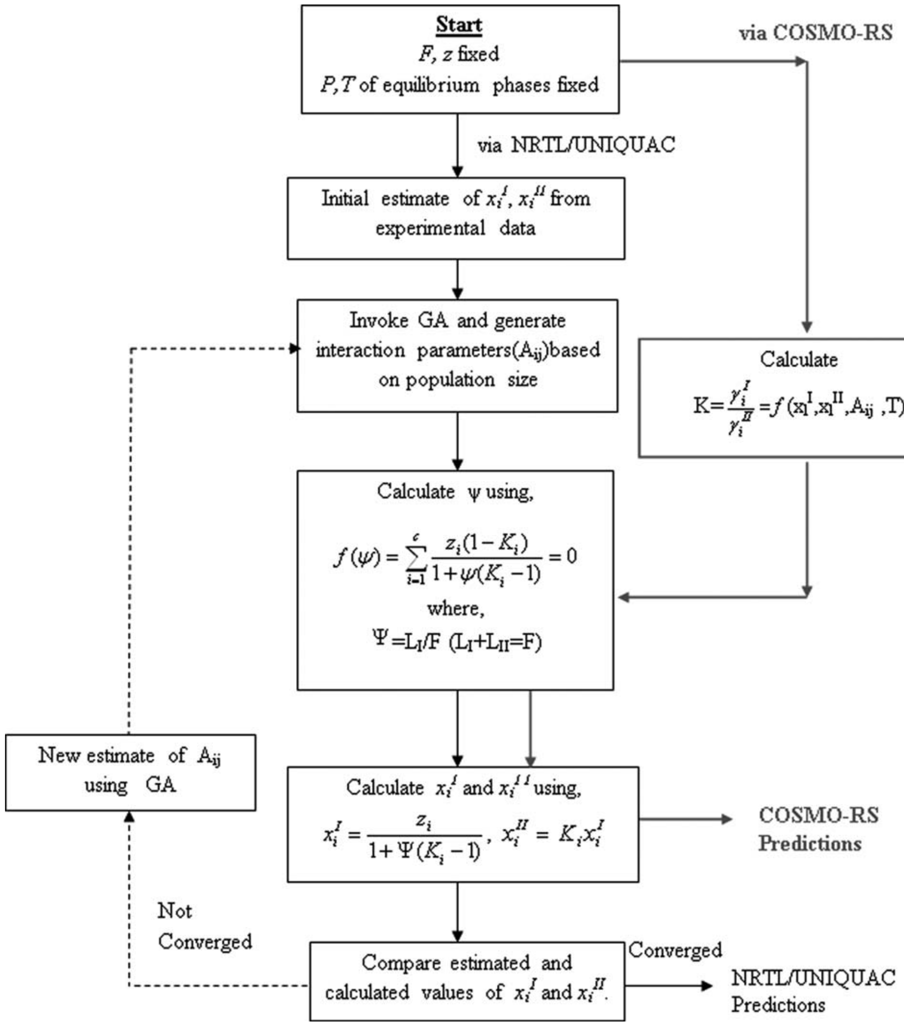

Figure 1. The modified Rashford–Rice algorithm[31] for NRTL/UNIQUAC/COSMO-RS predictions. (----- NRTL/UNIQUAC; ——— COSMO-RS)

ethyl sulfate [EMIM][EtSO$_4$] ($C_8H_{16}N_2O_4S$) of purity >99% were supplied by Sigma Aldrich, Germany. 1-ethyl-3-methylimidazolium methylsulphonate [EMIM][MeSO$_3$] ($C_8H_{16}N_2O_3S$) IL were purchased from Fluka with a purity of >99%. According to supplier, pyridine (C_5H_5N) and thiophene (C_4H_4S) obtained from Sigma Aldrich were indicated to posses mass fractions greater than 98%. Toluene (C_7H_8) was obtained form Merck with a purity of >99.5%. $CDCl_3$ of purity >99.8%, was used for the ^{1}H NMR analysis of the extract and raffinate phase compositions and was supplied by Sigma Aldrich, Germany. The chemical structures of the IL's are given in Table 1.

Desired amount of the four components were mixed in 15 mL stoppered bottle with the total volume of mixture fixed at 8 mL. The samples bottles were eventually sealed with parafilm tape to prevent any loss of the components due to evaporation. The bottles were then placed inside a water-shaker bath set at 100 rpm and at 298.15 K. Shaking were

Table 1. List of Ionic Liquids Studied in this Work

S. No	Formal Name	Acronym	Structure
1	1-ethyl-3-methylimidazolium acetate ($C_8H_{14}N_2O_2$)	[EMIM][OAc]	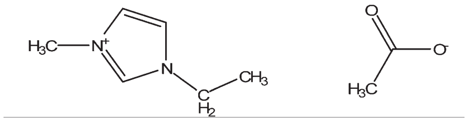
2	1-ethyl-3-methylimidazolium ethylsulfate ($C_8H_{16}N_2O_4S$)	[EMIM][EtSO$_4$]	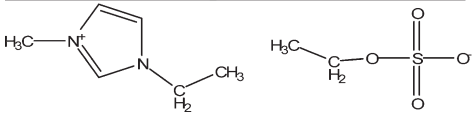
3	1-ethyl-3-methylimidazolium methylsulfonate ($C_7H_{14}N_2O_2$)	[EMIM][MeSO$_3$]	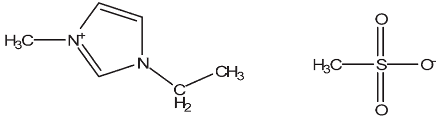

Table 2. NMR Peak Assignment for Quantitative Analysis in the Quaternary Mixture

Chemical Compound and Chemical Shifts in NMR Spectra (Relative to TMS)	
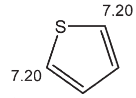 Thiophene	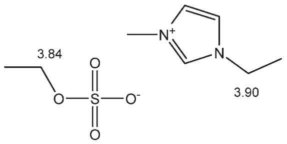 [EMIM][EtSO$_4$]
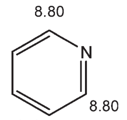 Pyridine	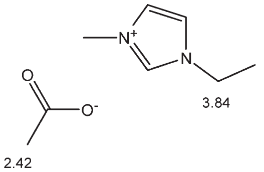 [EMIM][OAc]
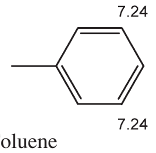 Toluene	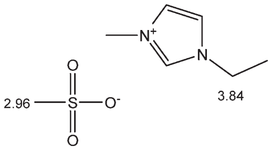 [EMIM][MeSO$_3$]

continued for 6 h in the thermostatic shaker bath (Dailhan Lab, China). Spring clamps were used so that the bottles are held on the tray. The temperature was kept within ±0.01 K. An overnight settling time of 12 h ensured that the two phases were in equilibrium.

Quantification of LLE data for quaternary systems was determined by the ^{1}H NMR of the phases in equilibrium. In recent times, ^{1}H NMR spectra is used for the determination of composition of phases at equilibrium.[39–44] The composition of these equilibrium phases was analyzed by NMR spectrometer of 11.74 Tesla (20 MHz response of ^{1}H). In this study, a small amount of each phase was dissolved in 0.5 mL of CDCl$_3$ in two different NMR (thrift Grade) tubes, which were sealed properly. The peak areas of the hydrogen atom of each component were obtained. From this data, we calculate the individual composition in both the phases. The aromatic ring structure of imidazolium, thiophene, pyridine, and toluene compounds show peak in the range of 6–9.5, whereas the methyl group of the cation/anion of IL show a peak between 3–4 (Table 2). The peak depends on the anion attached to the imidazolium cation. It should be noted that the peaks for thiophene, pyridine, and toluene are near to each other so equations[39–44] are formed by adding the respective areas of hydrogen and then solved simultaneously. Also, all the atom types of thiophene, pyridine, imidazolium ring, and toluene are aromatic in nature and more or less show in the same narrow range, that is, 7–9. So, we have added the areas of all the hydrogen atoms in such cases. The uncertainty of composition determination was checked by choosing known mixtures in the homogenous region close to the binodal curve and then obtaining their ^{1}H NMR. The measured results gave (+/−0.001 mole fraction) with the actual compositions.

Results and Discussion

LLE for the quaternary systems of 1-ethyl 3-methylimidazolium acetate (1) + thiophene (2) + pyridine (3) + toluene (4), 1-ethyl 3-methylimidazolium ethylsulfate (1) + thiophene (2) + pyridine (3) + toluene (4) and 1-ethyl- 3-methylimidazolium methylsulfonate (1) + thiophene (2) + pyridine (3) + toluene (4) were experimentally determined at 298.25 K. Tables 3–5 list the composition of the experimental tie lines for the three investigated systems at 298.15 K. It also shows the values of the selectivity (*S*) and distribution coefficient (*β*) which are used to characterize the suitability of a solvent in LLE. These parameters were calculated according to the following equations

$$S=\frac{x^{\mathrm{E}}_{\mathrm{TS/PY}}}{x^{\mathrm{R}}_{\mathrm{TS/PY}}}\times\frac{x^{\mathrm{R}}_{\mathrm{TO}}}{x^{\mathrm{E}}_{\mathrm{TO}}} \tag{5}$$

$$\beta=\frac{x^{\mathrm{E}}_{\mathrm{TS/PY}}}{x^{\mathrm{R}}_{\mathrm{TS/PY}}} \tag{6}$$

where x is the mole fraction, the superscript E and R refer to the extract and raffinate phase, respectively, and the subscripts TS, PY, and TO refers to thiophene, pyridine, and toluene, respectively.

Figures 2–4 shows the graphical representations of the tie-lines of three quaternary systems at 298.15 K. The evaluation of selectivity (*S*) and distribution coefficient (*β*) for each system as a function of mole fraction of thiophene(solute) and pyridine (solute) in the toluene rich phase are given in Tables 3–5. The dependence of selectivity values on IL concentration is very difficult to depict as the system has four components each interacting differently with IL. There may be formation of weak hydrogen bond in solution which cannot be explained by LLE data alone. However, it can be seen (Tables 3–5) that the selectivity values are higher when the mole fraction of either solute is very less. A similar behavior has been observed from the separation of aromatic and aliphatic compounds using IL.[39,45–47]

The distribution coefficient values for all the studied systems are given Tables 3–5. Among three imidazolium-based ILs, [EMIM][MeSO$_3$] (Table 5) is a potential IL where the

Table 3. Composition of Experimental Tie-Lines, Selectivity (*S*) and Distribution Ratio for [EMIM][OAc] (1) + thiophene (2) + pyridine (3) + toluene (4) at 298.15 K

	Ionic Liquid Rich Phase					Toluene Rich Phase					Selection Parameter			
	x_1^I	x_3^I	x_2^I	x_{23}^I	x_4^I	x_1^{II}	x_2^{II}	x_3^{II}	x_{23}^{II}	x_4^{II}	*S*th	*β*th	S_{pyr}	β_{pyr}
1	0.9017	0.0025	0.0791	0.0816	0.0167	0	0.047	0.0788	0.1259	0.8741	2.8	0.1	52.5	1.0
2	0.7511	0.1007	0.116	0.2167	0.0322	0	0.1859	0.0839	0.2698	0.7302	12.3	0.5	31.4	1.4
3	0.6843	0.1475	0.1277	0.2752	0.0405	0	0.2608	0.0919	0.3527	0.6473	9.0	0.6	22.2	1.4
4	0.6249	0.2295	0.0835	0.313	0.062	0	0.4504	0.0351	0.4854	0.5146	4.2	0.5	19.7	2.4
5	0.4675	0.3937	0.0693	0.4631	0.0695	0	0.7068	0.016	0.7228	0.2772	2.2	0.6	17.3	4.3
6	0.4078	0.4277	0.0875	0.5152	0.077	0	0.7829	0.0159	0.7988	0.2012	1.4	0.5	14.4	5.5
7	0.3418	0.4854	0.097	0.5824	0.0758	0	0.8698	0.0235	0.8933	0.1067	0.8	0.6	5.8	4.1
8	0.3138	0.5447	0.1149	0.6595	0.0267	0	0.9173	0.0241	0.9414	0.0586	1.3	0.6	10.5	4.8

Table 4. Composition of Experimental Tie-Lines, Selectivity (S) and Distribution ratio for [EMIM][EtSO$_4$] (1) + thiophene (2) + pyridine (3) + toluene (4) at 298.15 K

	Ionic Liquid Rich Phase					Toluene Rich Phase					Selection Parameter			
	x_1^I	x_3^I	x_3^I	x_{23}^I	x_4^I	x_1^{II}	x_2^{II}	x_3^{II}	x_{23}^{II}	x_4^{II}	S_{th}	βth	S_{pyr}	β_{pyr}
1	0.8583	0.0697	0.0066	0.0763	0.0654	0	0.0288	0.022	0.0508	0.9492	35.1	2.4	4.4	0.3
2	0.7527	0.142	0.0064	0.1484	0.0988	0	0.0998	0.0326	0.1324	0.8676	12.5	1.4	1.7	0.2
3	0.6981	0.1729	0.011	0.1839	0.118	0	0.1631	0.0461	0.2092	0.7908	7.1	1.1	1.6	0.2
4	0.6676	0.1898	0.0225	0.2123	0.12	0	0.2474	0.0584	0.3059	0.6941	4.4	0.8	2.2	0.4
5	0.5582	0.2439	0.0565	0.3004	0.1414	0	0.3079	0.0714	0.3793	0.6207	3.5	0.8	3.5	0.8
6	0.5019	0.2892	0.0641	0.3533	0.1447	0	0.364	0.0759	0.4398	0.5602	3.1	0.8	3.3	0.8
7	0.4477	0.327	0.0776	0.4046	0.1477	0	0.4175	0.1192	0.5367	0.4633	2.5	0.8	2.0	0.7
8	0.2869	0.456	0.078	0.534	0.1791	0	0.5141	0.124	0.6381	0.3619	1.8	0.9	1.3	0.6

Table 5. Composition of Experimental Tie-Lines, Selectivity (S) and Distribution Ratio for [EMIM][MeSO$_3$] (1) + thiophene (2) + pyridine (3) + toluene (4) at 298.15 K

	Ionic Liquid Rich Phase					Toluene Rich Phase					Selection Parameter			
	x_1^I	x_3^I	x_3^I	x_3^I	x_4^I	x_1^{II}	x_2^{II}	x_3^{II}	x_{23}^{II}	x_4^{II}	S_{th}	β_{th}	S_{pyr}	β_{pyr}
1	0.9145	0.0375	0.0235	0.061	0.0245	0	0.1245	0.0305	0.155	0.845	10.4	0.3	26.6	0.8
2	0.7966	0.0928	0.0577	0.1505	0.0529	0	0.1974	0.0915	0.2889	0.7111	6.3	0.5	8.5	0.6
3	0.7222	0.1131	0.0801	0.1933	0.0845	0	0.2491	0.1005	0.3496	0.6504	3.5	0.5	6.1	0.8
4	0.6281	0.2022	0.0658	0.2681	0.1038	0	0.3284	0.0986	0.427	0.573	3.4	0.6	3.7	0.7
5	0.5507	0.2382	0.0915	0.3296	0.1197	0	0.441	0.1066	0.5476	0.4524	2.0	0.5	3.2	0.9
6	0.4391	0.3249	0.1123	0.4372	0.1237	0	0.4665	0.1292	0.5957	0.4043	2.3	0.7	2.8	0.9
7	0.3653	0.3706	0.1368	0.5075	0.1272	0	0.5146	0.14	0.6546	0.3454	2.0	0.7	2.7	1.0
8	0.3205	0.4043	0.1496	0.5539	0.1255	0	0.5771	0.1487	0.7258	0.2742	1.5	0.7	2.2	1.0

distribution coefficient values for both thiophene and pyridine are less than unity at all compositions. The distribution coefficient of [EMIM][OAc] is less than unity for thiophene but very high for pyridine. On the contrary, [EMIM][EtSO$_4$] shows high values for thiophene but low values for pyridine (Table 4). Thermodynamically, an extracting solvent must exhibit high selectivity and distribution coefficient. The selectivity values do not seem too much contribute as the values are close to each other for both thiophene and pyridine(Tables 3–5).The only values which are higher are the ones observed for pyridine in [EMIM][OAc](Table 3). Thus, the results shows that that [EMIM][MeSO$_3$] looks to be the promising IL for the simultaneous separation process.

The NRTL and UNIQUAC models were used to correlate the experimental tie-line compositions. The ternary diagram with the tie lines for each system is plotted in Figures 2–4 for NRTL and Figures 5–7 for UNIQUAC model. The figure provides a clear visualization of the change in the size and shape of the immiscibility region as a result of the increase in solute concentration in the toluene rich phase. It is seen that the tie-line length is significantly large. Therefore, the immiscibility of solute (thiophene + pyridine) + ILs pairs are very high at 298.15 K. It is also observed that the tie lines show a positive slope at bottom of triangular diagram, while showing negative slope in other regions. The sign of the tie-

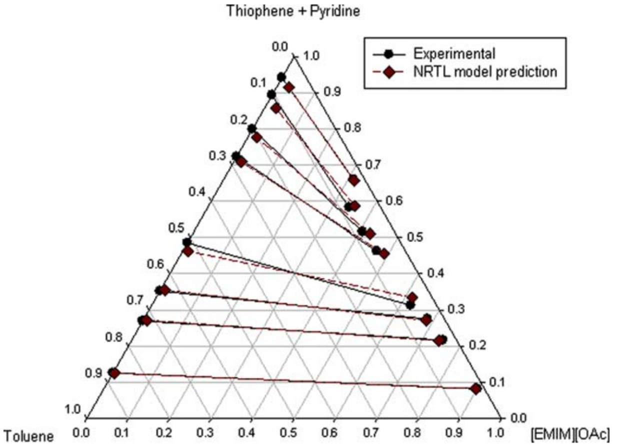

Figure 2. Experimental and NRTL predicted tie lines for the quaternary system: [EMIM][OAc] (1) + thiophene (2) + pyridine (3) + toluene (4) at T = 298.15 K.

[Color figure can be viewed in the online issue, which is available at wileyonlinelibrary.com.]

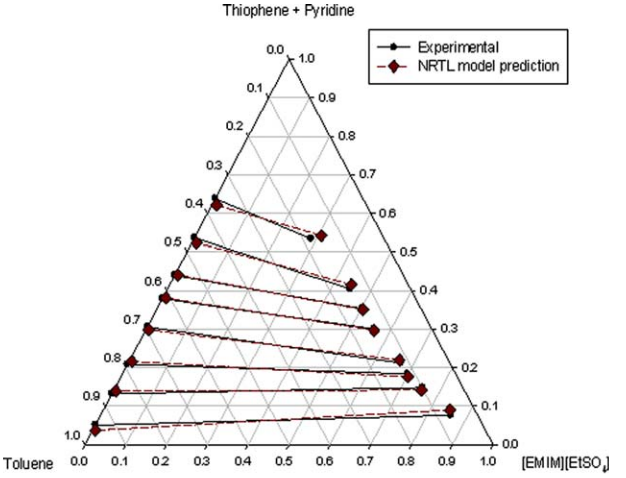

Figure 3. Experimental and NRTL predicted tie lines for the quaternary system: [EMIM][EtSO$_4$] (1) + thiophene (2) + pyridine (3) + toluene (4) at T = 298.15 K.

[Color figure can be viewed in the online issue, which is available at wileyonlinelibrary.com.]

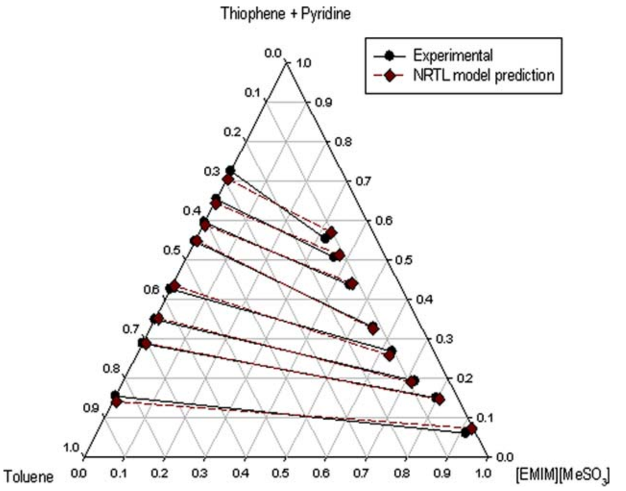

Figure 4. Experimental and NRTL predicted tie lines for the quaternary system: [EMIM][EtSO$_4$] (1) + thiophene (2) + pyridine (3) + toluene (4) at T = 298.15 K.

[Color figure can be viewed in the online issue, which is available at wileyonlinelibrary.com.]

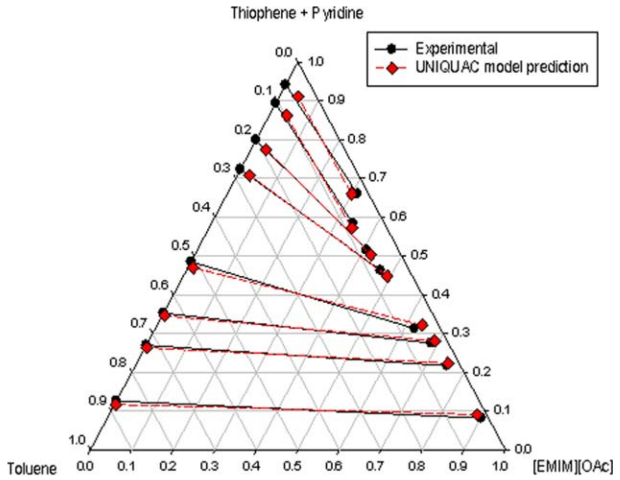

Figure 6. Experimental and UNIQUAC predicted tie lines for the quaternary system: [EMIM][EtSO$_4$] (1) + thiophene (2) + pyridine (3) + toluene (4) at T = 298.15 K.

[Color figure can be viewed in the online issue, which is available at wileyonlinelibrary.com.]

line slope change also depends on the type of molecular interaction. For example, the ternary system of {n-Hexane + pyridine + IL} shows a positive slope,[13] whereas {hexadecane +pyridine + methanol}[48] exhibits a negative slope. In addition, the ternary systems: {nonane + benzene + [BMIM][PF$_6$]}, {nonane + toluene + [BMIM][PF$_6$]}, and {undecane + toluene + [BMIM][PF$_6$]} shows both positive and negative slope in the triangular diagram.[49] An important observation from Figures 2–4 indicates that the mole fraction of IL in raffinate phase is zero. This indicates the IL will not contaminate the diesel phase. The negative slope implies higher quantity of IL. It should be noted that the practical application of simultaneous desulfurization and denitrification of diesel oil corresponds to low concentration of sulfur- and nitrogen-containing compounds. Therefore, the lowest part of the triangular diagrams must be considered for practical separation region in all the diagrams.

A comparison of selectivity and distribution with the mole fraction of hydrocarbon in hydrocarbon rich phase is given in Table 6. It gives the values with the potential IL namely [EMIM][MeSO$_3$] with various component of diesel namely pentane(parrafin),[50]isooctane (isoparaffin),[44] cylohexane (napthene),[51] and toluene(aromatic). From Table 6, it is clear that the selectivities are the highest for pentane followed by toluene, cyclohexane, and isooctane. A remarkable fact is that the distribution coefficient is lesser than one for all the individual diesel component. This make solvent recycle easier with lesser requirement of number of theoretical stages.

The difference between experimental and predicted tie-line composition were minimized using objective function (Eq. 1) and then used to calculate the RMSD values (Eq. 4).

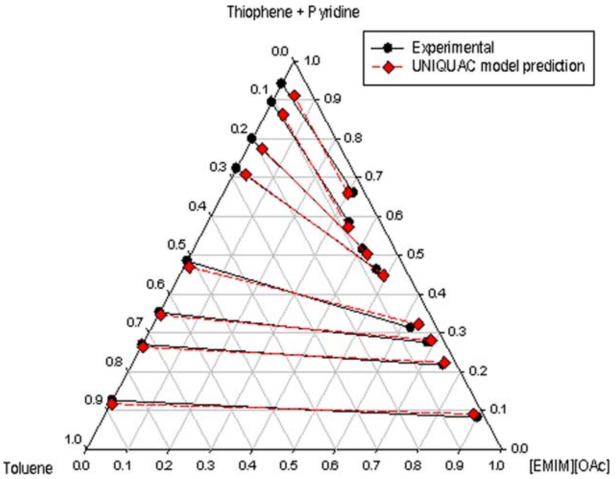

Figure 5. Experimental and UNIQUAC predicted tie lines for the quaternary system: [EMIM][OAc] (1) + thiophene (2) + pyridine (3) + toluene (4) at T = 298.15 K.

[Color figure can be viewed in the online issue, which is available at wileyonlinelibrary.com.]

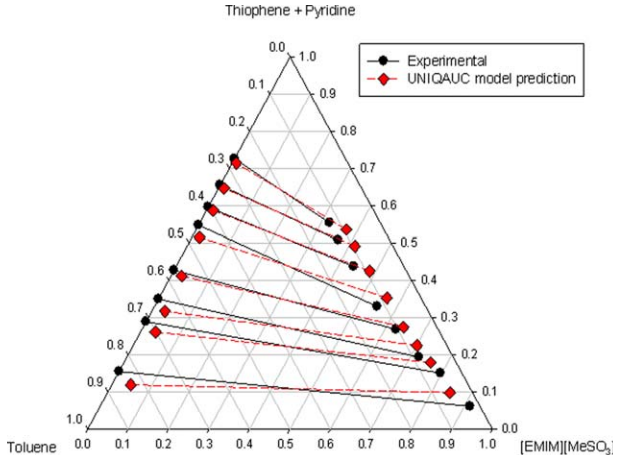

Figure 7. Experimental and UNIQUAC predicted tie lines for the quaternary system: [EMIM][EtSO$_4$] (1) + thiophene (2) + pyridine (3) + toluene (4) systems at T = 298.15 K.

[Color figure can be viewed in the online issue, which is available at wileyonlinelibrary.com.]

Table 6. Comparison of Selectivity and Capacity of [EMIM][$MeSO_3$] with Various Components of Diesel

	Pentane[50]		Cyclohexane[51]		Isooctane[44]		Toluene (This Work)	
x[a]	S_{23}	β_{23}	S_{23}	β_{23}	S_{23}	β_{23}	S_{23}	β_{23}
0.873	1352.01	0.74	8.31	0.56	4.36	0.39	13.60	0.40
0.783	296.22	0.75	3.84	0.71	3.63	0.60	7.00	0.50
0.715	117.72	0.57	3.43	0.74	2.77	0.53	4.30	0.60
0.608	12.24	0.53	2.44	0.60	3.05	0.73	3.50	0.60
0.500	5.66	0.84	2.38	0.70	2.57	0.79	2.30	0.60
0.423	5.52	0.63	1.89	0.71	1.77	0.74	2.40	0.70
0.344	3.50	0.93	1.53	0.71	1.31	0.75	2.10	0.80
0.277	2.53	0.90	1.53	0.71	1.15	0.81	1.70	0.80

[a]Average mole fraction of hydrocarbon in raffinate phase.

In case of UNIQUAC model, the van der Waals parameters such as r and q were calculated according to the literature,[32] and are given in Table 7. The observed RMSD values for three quaternary systems are listed in Tables 8–10. The RMSD values are lesser than unity for all the studied system which indicates a high degree of accuracy. The binary interaction parameters and the corresponding objective function value of the quaternary systems are also listed in Tables 7–9.

Table 7. UNIQUAC Structural Parameters for the Different Compounds in the LLE System

Component	r	q
1-ethyl-3-methylimidazolium acetate[a]	8.7500	5.5600
1-ethyl-3-methylimidazolium ethyl sulfate[a]	8.3927	6.6260
1-ethyl-3-methylimidazolium methylsulfonate[a]	8.14	6.08
Thiophene	2.8569	2.140
Pyridine	2.9993	2.113
Toluene	3.9228	2.968

[a]Calculated via Ref. 32

The obtained interaction parameters can be used for the design and simulation of extraction column for the simultaneous separation of thiophene and pyridine from diesel oil.

The COSMO-RS predicted tie lines are given in Figures 8–10. The tie lines are agreeing each other qualitatively, whereas length and shape of the immiscible region has a bit deviation, particularly in IL rich phase. However, COSMO-RS was not able to predict the change of sign of the tie line in these systems at low solutes concentration. It should be noted that ILs are depicted as hydrogen-bonded polymeric molecules of the type $[(RMIM)_x(X)_{x-n}]_n+$ $[(RMIM)_{x-n}(X)_x]_n^-$ where RMIM is the 1,3-dialkylimidazolium cation and X is the anion.[52,53] Accommodation of aromatic molecules implies a disruption of the hydrogen bond network where inclusion-type compounds can be formed.[54] The polymeric nature of the IL is still present when they are mixed with aromatic components. IL/aromatic mixtures are known to form liquid clathrates. For example, in the case of [RMIM][PF_6]/benzene mixture, the inclusion compound $[([RMIM][PF_6])_2(benzene)]n$ could be trapped and can be

Table 8. NRTL and UNIQUAC Interaction Parameters for the [EMIM][OAc] (1) + thiophene (2) + pyridine (3) + toluene (4) Systems at T = 298.15 K

	NRTL Model Parameters				UNIQUAC Model Parameters			
$i-j$	τ_{ij}/J mole^{-1}	τ_{ji}/J mole^{-1}	F[a]	RMSD[b]	A_{ij}/J mole^{-1}	A_{ji} /J mole^{-1}	F[a]	RMSD[b]
System: [EMIM][CH_3COO] (1) + thiophene (2) +pyridine (3) + toluene (4)								
1–2	8147.2	798.5	-9.71×10^{-3}	0.009268	628	567.34	-15.57×10^{-3}	0.015493
1–3	1187.8	7108.1			847.04	−28.8211		
1–4	1603	369.69			271.21	1185.2		
2–3	975.68	8323.8			−34.06	149.41		
2–4	1542.7	−0.4032			947.97	211.46		
3–4	684.87	3393.2			301.23	1326.3		

[a]Calculated using Eq. 1.
[b]Calculated using Eq. 4.

Table 9. NRTL and UNIQUAC Interaction Parameters for the [EMIM][$EtSO_4$] (1) + thiophene (2) + pyridine (3) + toluene (4) Systems at T = 298.15 K

	NRTL Model Parameters				UNIQUAC Model Parameters			
$i-j$	τ_{ij}/J mole^{-1}	τ_{ji}/J mole^{-1}	F[a]	RMSD[b]	A_{ij} /J mole^{-1}	A_{ji} /J mole^{-1}	F[a]	RMSD[b]
System: [EMIM][$EtSO_4$] (1) + thiophene (2) + pyridine (3) + toluene (4)								
1–2	8147.2	798.87	-9.71×10^{-3}	0.012318	628	567.34	-15.36×10^{-3}	0.015493
1–3	1187.8	7108.1			847.04	−28.821		
1–4	1603	369.69			271.21	1185.2		
2–3	975.68	8323.8			−34.06	149.41		
2–4	1542.7	−0.40326			947.97	211.46		
3–4	684.87	3393.2			301.23	1326.3		

[a]Calculated using Eq. 1.
[b]Calculated using Eq. 4.

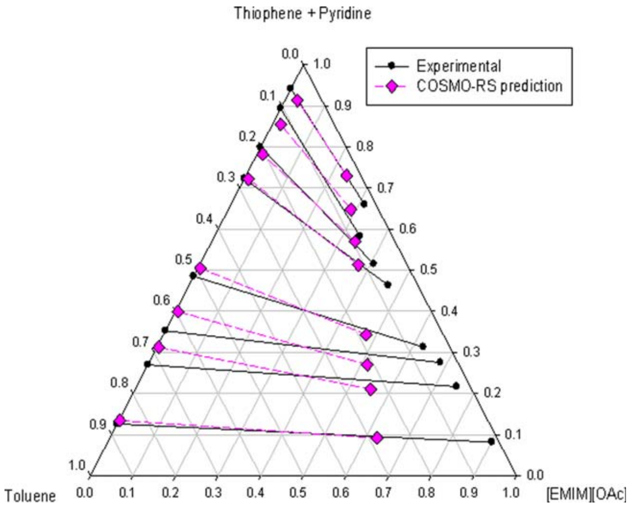

Figure 8. **Experimental and COSMO-RS predicted tie lines for the quaternary system:[EMIM][OAc] (1) + thiophene (2) + pyridine (3) + toluene (4) at T = 298.15 K.**

[Color figure can be viewed in the online issue, which is available at wileyonlinelibrary.com.]

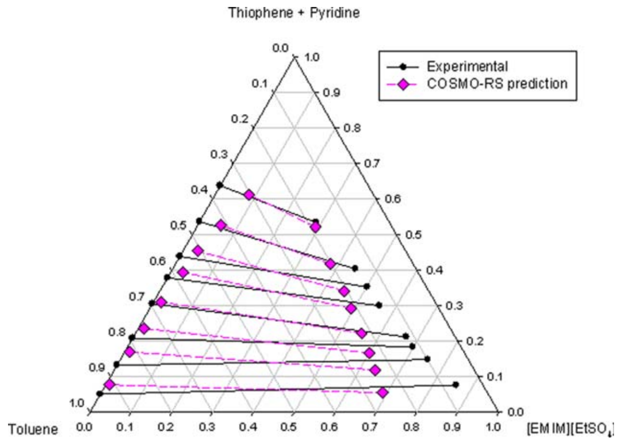

Figure 9. **Experimental and COSMO-RS predicted tie lines for the quaternary system: [EMIM][EtSO$_4$] (1) + thiophene (2) + pyridine (3) + toluene(4) at T = 298.15 K.**

[Color figure can be viewed in the online issue, which is available at wileyonlinelibrary.com.]

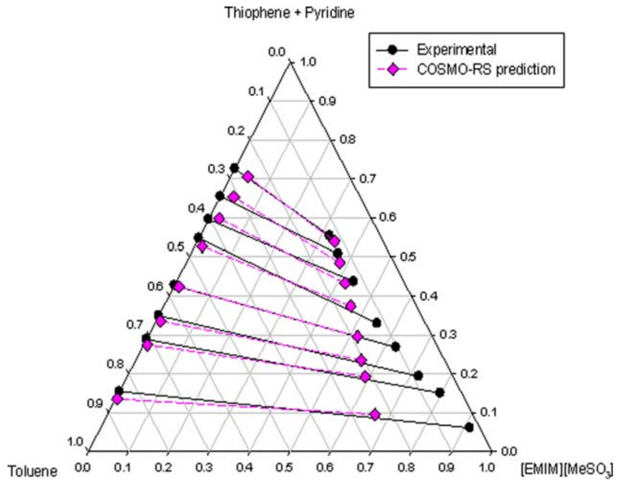

Figure 10. **Experimental and COSMO-RS predicted tie lines for the quaternary system: [EMIM][EtSO$_4$] (1) + thiophene (2) + pyridine (3) + toluene (4) at T = 298.15 K.**

[Color figure can be viewed in the online issue, which is available at wileyonlinelibrary.com.]

observed via its X-ray structure.[55] In the case of unimolecular COSMO calculation, screening charges are computed by placing a single molecule in the midst of an infinite conductor. Thus, an estimation of hydrogen bond energy which originates from a network is lost. Despite of this fact the prediction of COSMO-RS is appreciably good considering the method to be unimolecular. The aromatic compounds (pyridine/thiophene) interacts via CH (imidazolium)—π bonds(aromatic).In the case of IL, it stabilizes itself with respect to the C$_2$—X hydrogen bonding (X = [MeSO$_3$]/[OAc]/[EtSO$_4$])(here 2 refers to the carbon atom between the two nitrogen atoms of the imidazolium ring) .Thus, there is a competing effect between CH-π interaction and the hydrogen bonding interaction. It should be assumed that for [MeSO$_3$] anion the C$_2$—X hydrogen bonding is less dominating as compared to the intramolecular hydrogen bonding. This results in a higher selectivity.

The entire model is characterized by our earlier COSMO-RS parameters,[24] $a_{\text{eff}} = 6.32$ Å^2 (surface area of a standard segment), $\alpha' = 8419$ kcal Å^4 mol^{-1} e^{-2} (misfit energy constant) for misfit energy interaction, $c_{\text{hb}} = 75006$ kcal Å^4 mol^{-1} e^{-2} (hydrogen bonding energy constant), and $\sigma_{\text{hb}} = 0.0084$ e Å^{-2} (hydrogen bonding cutoff). No change in the parameters was made to predict the quaternary systems. On way to

Table 10. NRTL and UNIQUAC Interaction Parameters for the [EMIM][MeSO$_3$] (1) + thiophene (2) + pyridine (3) + toluene(4) Systems at T = 298.15 K

	NRTL Model Parameters				UNIQUAC Model Parameters			
$i-j$	τ_{ij}/J mole^{-1}	τ_{ji}/J mole^{-1}	F^{a}	RMSD^{b}	A_{ij}/J mole^{-1}	A_{ji}/J mole^{-1}	F^{a}	RMSD^{b}
System: [EMIM][MeSO$_3$] (1) + thiophene (2) + pyridine (3) + toluene (4)								
1–2	1087.3	7365.9	-5.63×10^{-3}	0.009375	−67.256	238.13	-35.3×10^{-3}	0.023485
1–3	6576.8	113.74			638.49	2710		
1–4	5714.5	12788			373.86	2668		
2–3	14999	1242.2			806.65	−57.081		
2–4	336.13	867.22			25.911	−179.68		
3–4	14938	6377			978.09	975.95		

[a] Calculated using Eq. 1.
[b] Calculated using Eq. 4.

correct, the deviation is to account for the cross hydrogen bonding by defining suitable hydrogen bonding cutoff from experimental data. The RMSD for the systems obtained were 8.41, 8.74, and 6.53% for [OAc],[$EtSO_4$], and [$MeSO_3$], respectively.

Conclusions

LLE data for the quaternary system containing [EMIM][OAc],[EMIM][$EtSO_4$], and [EMIM][$MeSO_3$] with thiophene, pyridine, and toluene were experimentally determined at 298.15 K. In general, the tie lines show a positive slope at bottom of triangular diagram and negative slope elsewhere. In terms of selectivity and distribution coefficient values, [EMIM][$MeSO_3$] looks to be the promising IL for the simultaneous separation of sulfur and nitrogen from diesel oil at 298.15 K. In addition, the degree of consistency of the tie line was validated by NRTL and UNIQUAC models. The COSMO-RS based approach has been applied to predict the tie lines of quaternary system containing IL's with reasonable accuracy. The COSMO-RS predicted RMSD for the systems were 8.41, 8.74, and 6.53% for [OAc], [$EtSO_4$], and [$MeSO_3$], respectively.

Acknowledgment

The authors are grateful to the Department of Science and Technology (DST), Government of India for the financial support through project SR/FTP/08-08 under the Fast Track Scheme.

Notation

Latin symbols

[EMIM] = cation: 1-ethyl 3-methylimidazolium
[OAc] = anion: acetate
[$EtSO_4$] = anion: ethyl sulphate
[$MeSO_3$] = anion: methylsulphonate
S = selectivity
F = objective function
$RMSD$ = root mean square deviation
a_{eff} = effective segment surface area, Å^2
c_{hb} = misfit energy constant, kcal Å^4 mol^{-1} e^{-2}
$p_i(\sigma)$ = sigma profile of component i i.e. probability of segment i having a charge density σ
R = universal gas constant, J K^{-1} mol^{-1}
T = temperature, K
r = pure component volume parameter
q = pure component surface area parameter
m = number of tie lines
c = number of components in the LLE system
z = coordination number = 10
g_{ji} = average interaction energy for the interaction of molecules of component j with molecules of component i

Greek letters

α' = misfit energy constant, kcal Å^4 mol^{-1} e^{-2}
σ_{hb} = hydrogen bonding cutoff value, e Å^{-2}
β = distribution coefficient
τ = NRTL interaction parameter
α = NRTL nonrandomness parameter

Literature Cited

1. Anantharaj R, Banerjee T. Evaluation and comparison of global scalar properties for the simultaneous interaction of ionic liquids with thiophene and pyridine. *Fluid Phase Equilib.* 2010;293:22–31.
2. Zhang S, Zhang Q, Zhang ZC. Extractive desulphurization and denitrification of fuels using ionic liquids. *Ind Eng Chem Res.* 2004;43:617–622.
3. Zhao D, Sun Z, Li F, Liu R, Shan H. Oxidative desulphurization of thiophene catalyzed by $(C_4H_9)_4NBr.2C_6H_{11}NO$ coordinated ionic liquid. *Energy Fuels.* 2008;22:3065–3069.
4. Hansmeier AR, Meindersma GW, Haan AB. Desulfurization and denitrogenation of gasoline and diesel fuels by means of ionic liquids. *Green Chem.* 2011;13:1907–1913.
5. Berresheim H. Distribution of atmospheric sulphur species over various wetland regions in the southeastern USA. *Atmos Environ Part A.* 1993;27:211–221.
6. Jeon HJ, Ko CH, Kim SH, Kim JN. Refractory sulphur compounds in diesel oil using activated compounds with controlled porosity. *Energy Fuels.* 2009;23:2537–2543.
7. Alonsa L, Arce A, Francisco M, Rodriguez O, Soto A. Gasoline desulphurization using extraction with [C_8mim][BF_4] ionic liquid. *AIChE J.* 2007;53:3108–3115.
8. Jayaraman A, Yang FH, Yang RT. Effect of nitrogen compounds and polyaromatic hydrocarbons on desulphurization of liquid fuels by adsorption via π-complexation with Cu(I)Y Zeolite. *Energy Fuels.* 2006;20:909–914.
9. Anantharaj R, Banerjee T. COSMO-RS-based screening of ionic liquids as green solvents in denitrification studies. *Ind Eng Chem Res.* 2010;49:8705–8725.
10. Varma NR, Anantharaj R, Banerjee T. Experiments correlations and cosmo-rs predictions for the extraction of benzothiophene from n-hexane using imidazolium-based ionic liquids. *Chem Eng J.* 2011;166:30–39.
11. Anantharaj R, Banerjee T. COSMO-RS based predictions for the desulphurization of diesel oil using ionic liquids: effect of cation and anion combination. *Fuel Process Technol.* 2010; 92:20–39.
12. Ravilla UK, Banerjee T. Liquid liquid equilibria of imidazolium based ionic liquid + pyridine + hydrocarbon at 298.15 K: experiments and correlations. *Fluid Phase Equilib.* 2012;324:17–27.
13. Luisa Alonso L, Alberto Arce A, Francisco M, Soto A. Extraction ability of nitrogen-containing compounds involved in the desulfurization of fuels by using ionic liquids. *J Chem Eng Data.* 2010;55:3262–3267.
14. Kedra-Krolik K, Mutelet F, Jaubert J. Extraction of thiophene or pyridine from n-Heptane using ionic liquids gasoline and diesel desulfurization. *Ind Eng Chem Res.* 2011;50:2296–2306.
15. Schmitz C, Datsevitch L, Jess A. Deep desulphurization of diesel oil: kinetic studies and process-improvement by the use of a two-phase reactor with pre-saturator. *Chem Eng Sci.* 2004;59:2821–2829.
16. Xie LL, Reguillon AF, Rostaing SP, Wang XX, Fu X, Estager J, Vrinat M, Lemaire M. Selective extraction and identification of neutral nitrogen compounds contained straight-run diesel feed using chloride based ionic liquid. *Ind Eng Chem Res.* 2008;47:8801–8807.
17. Anantharaj R, Banerjee T. Quantum chemical studies on the simultaneous interaction of thiophene and pyridine with ionic liquid. *AIChE J.* 2010;57:749–764.
18. Ramirez S, Carbrera C, Aguilar C, Vaca H, Vega P, Agueda R, Garcia A, Santiago R, Schacht P. Two stages light gas oil hydrotreating for low sulphur diesel oil production. *Catal Today.* 2004;98:323–332.
19. Nie Y, Li C, Meng H, Wang ZN. N-dialkylimidazolium dialkylphosphate ionic liquids: their extractive performance for thiophene series compounds from fuel oils versus the length of alkylgroup. *Fuel Process Technol.* 2008;89:978–983.
20. Anugwom I, Mäki-Arvela P, Salmi T, Mikkola J. Ionic liquid assisted extraction of nitrogen and sulphur-containing air pollutants from model oil and regeneration of the spent ionic liquid. *J Environ Prot.* 2011;2:796–802.
21. Mochizuki Y, Sugawara K. Removal of organic sulfur from hydrocarbon resources using ionic liquids. *Energy Fuels.* 2008;22:3303–3307.
22. Eber J, Wasserscheid P, Jess A. Deep desulfurization of oil refinery streams by extraction with ionic liquids. *Green Chem.* 2004;6:316–322.
23. Domanska U, Laskowska M, Marciniak A. Phase equilibria of (1-ethyl-3-methylimidazolium ethylsulfate + hydrocarbon, + ketone, and + ether) binary systems. *J Chem Eng Data.* 2008;53:498–502.
24. Anantharaj R, Banerjee T. Fast solvent screening for the simultaneous hydrodesulphurization and hydrodenitrification of diesel oil using ionic liquids. *J Chem Eng Data.* 2011;56:2770–2785.
25. Kumar AP, Banerjee T. Thiophene separation with ionic liquids for desulphurization: a quantum chemical approach. *Fluid Phase Equilib.* 2009;278:1–8.

26. Renon H, Prausnitz JM. Local compositions in thermodynamic excess functions for liquid mixtures. *AIChE J*. 1968;14:135–144.
27. Abrams DS, Prausnitz JM. Statistical thermodynamics of liquid mixtures: a new expression for the excess Gibbs energy of partly or completely miscible systems, *AIChE J*. 1975;21:116–128.
28. Banerjee T, Verma KK, Khanna A. Liquid-liquid equilibrium for ionic liquid systems using COSMO-RS: effect of cation and anion dissociation. *AIChE J*. 2008;54:1874–1885.
29. MATLAB GA Toolbox, Available at www.ise.ncsu.edu/kay/gaotv5.-zip, accessed on March 15, 2011.
30. Banerjee T, Singh MK, Khanna A. Genetic algorithm to estimate interaction parameters of multicomponent systems for liquid–liquid equilibria. *Comput Chem Eng*. 2005;29:1712–1719.
31. Seader JD, Henley EJ. Separation Process Principles, 2nd ed. New York: Wiley, 2005.
32. Banerjee T, Singh MK, Sahoo RK, Khanna A. Volume, surface and UNIQUAC interaction parameters for imidazolium based ionic liquids via polarizable continuum model. *Fluid Phase Equilib*. 2005; 234:64–76.
33. Klamt A, Schüürmann G. COSMO: a new approach to dielectric screening in solvents with explicit expressions for the screening energy and its gradient. *J Chem Soc Perkin Trans I*. 1993;2:799–805.
34. Klamt A. COSMO-RS: From Quantum Chemistry to Fluid Phase Thermodynamics and Drug Design, 1st ed. Amsterdam: Elsevier Science, 2005.
35. Banerjee T, Singh MK, Khanna A. Prediction of binary VLE for imidazolium based ionic liquid systems using COSMO-RS. *Ind Eng Chem Res*. 2006;45:3207–3219.
36. Banerjee T, Sahoo RK, Rath SS, Kumar P, Khanna A. Multicomponent liquid-liquid equilibria prediction of aromatic extraction systems using COSMO-RS. *Ind Eng Chem Res*. 2007;46:1292–1304.
37. Banerjee T, Khanna A. Infinite dilution activity coefficients for trihexyltetradecyl phosphonium ionic liquids: measurements and COSMO-RS prediction. *J Chem Eng Data*. 2006;51:2170–2177.
38. Diedenhofen M, Klamt A. COSMO-RS as a tool for property prediction of IL mixtures - a review. *Fluid Phase Equilib*. 2010;294:31–38.
39. Arce A, Earle MJ, Rodr'ıguez H, Seddon KR. Separation of benzene and hexane by solvent extraction with 1-alkyl-3-methylimidazolium bis*{*(trifluoromethyl) sulfonyl*}*amide ionic liquids: effect of the alkyl-substituent length. *J Phys Chem B*. 2007;111:4732–4736.
40. Arce A, Earle MJ, Rodr'ıguez H, Seddon KR. Separation of aromatic hydrocarbons from alkanes using the ionic liquid 1-ethyl-3-methylimidazolium bis{(trifluoromethyl) sulfonyl}amide. *Green Chem*. 2007;9:70–74.
41. Arce A, Earle MJ, Rodr'ıguez H, Seddon KR. Bis{(trifluoromethyl) sulfonyl}amide ionic liquids as solvents for the extraction of aromatic hydrocarbons from their mixtures with alkanes: effect of the nature of the cation. *Green Chem*. 2009;11:365–372.
42. Potdar S, Anantharaj R, Banerjee T. Aromatic extraction using mixed ionic liquids: experiments and COSMO-RS predictions. *J Chem Eng Data*. 2012;57;1026–1035.
43. Saikiran C, Banerjee T. Liquid liquid equilibrium data for 1-ethyl-3-methylimidazolium acetate - thiophene - diesel compound: experiments and correlations. *J Solution Chem*. 2012;41:898–913.
44. Anantharaj R, Banerjee T. Liquid-liquid equilibria for quaternary systems of imidazolium based ionic liquid + thiophene + pyridine + iso-octane at 298.15 K: experiments and quantum chemical predictions. *Fluid Phase Equilib*. 2011;312: 20–30.
45. Gonzalez EJ, Calvar N, Gomez E, Domlnguez A. Separation of benzene from linear alkanes (C_6-C_9) using 1-ethyl-3-methylimidazolium ethylsulfate at $T = 298.15$ K. *J Chem Eng Data*. 2010;55:3422–3427.
46. Gonzalez EJ, Calvar N, Gomez E, Domlnguez A. Liquid−liquid equilibria of the ternary systems of alkane + aromatic + 1-ethylpyridinium ethylsulfate ionic liquid at $T = (283.15$ and $298.15)$ K. *J Chem Eng Data*. 2010;55:5169–5175.
47. Meindersma GW, Hansmeier AR, Haan B. Ionic liquids for aromatics extraction. *present status and future outlook. Ind Eng Chem Res*. 2010;49:7530–7540.
48. Won DB, Park SJ, Han KJ, Kim CJ. Liquid-liquid equilibria for methanol + hexadecane +heterocyclic nitrogen –containing compounds at 298.15 K. *Fluid Phase Equilib*. 2002;193:217–227.
49. Maduro RM, Aznar M. Liquid-liquid equilibrium of ternary systems 1-butyl-3-methylimidazolium hexafluorophosphate +aromatic +aliphatic. *Fluid Phase Equilib*. 2010;265:129–138.
50. Anantharaj R, Banerjee T. Liquid-liquid equilibrium studies on the simultaneous removal of thiophene and pyridine from pentane using imidazolium based ionic liquids. *J Chem Eng Data*. 2013;58:829–837.
51. Shah M, Anantharaj R, Banerjee T, Yadav GD. Quaternary liquid-liquid equilibria for systems of imidazolium based ionic liquid- + thiophene + pyridine + cyclohexane at 298.15 K: experiments and quantum chemical predictions. *J Chem Thermodyn*. 2013;62:142–150.
52. Dupont J. On the solid, liquid and solution structural organization of imidazolium ionic liquids. *J Braz Chem Soc*. 2004;15:341–350.
53. Lopes J, Padua AAH. Nanostructural organization in ionic liquids. *J Phys Chem B* 2006;110:3330–3335.
54. Dupont J, Suarez PAZ. Physico-chemical processes in imidazolium ionic liquids. *Phys Chem Chem Phys*. 2006;8:2441–2452.
55. Holbrey JD, Reichert WM, Nieuwenhuyzen M, Sheppard O, Hardacre C, Rogers RD. Liquid clathrate formation in ionic liquid-aromatic mixtures. *Chem Commun*. 2003;4:476–477.

Manuscript received Oct. 30, 2012, revision received May 27, 2013, and fnial revision received Aug. 17, 2013.